Increased Secretion of Neuronal Exosome under Elevated Neuronal Activity

A thesis submitted by

Qiyi Li

in partial fulfillment of the requirements for the degree of

Master of Science

in

Pharmacology and Drug Development

Tufts University

Graduate School of Biomedical Sciences

May 2023

Advisor: Yongjie Yang, Ph.D

Abstract

Communication between neurons and astrocytes plays an essential role in supporting nervous system development and synaptic function. Neurons regulate astrocyte differentiation through Notch signaling during development, while astrocytes respond to pre-synapse released neurotransmitters like glutamate in response to the elevation of cytosolic Ca^{2+}. Dysfunctional protection from astrocyte can lead to excitotoxicity, contributing to neurodegenerative diseases. Exosomes, a subtype of extracellular vesicles sourced from intraluminal vesicles, have been studied as noninvasive delivery vehicles for biomolecules across the blood-brain barrier contributing to synapse support, neurite growth and removal, axon regeneration, and neurotransmitter production and recycling. In neuron-to-astrocyte communication, neuronal exosomes internalized by astrocytes play the role in translocating distinctive cargos like miR-124-3p into astrocytes benefiting upregulation of GLT-1 expression and protect synapses from excess glutamate. While studies have shown that synaptic glutamatergic activity influences neuronal exosome secretion in vitro, in situ exosomal signaling between neurons and astrocytes in the CNS remains unexplored. In this study, we utilized cell-type-specific exosome-and-astrocyte-reporter mice CD63-GFP$^{f/+}$, together with chemogenetic technology, to investigate exosome secretion after manipulating neuronal activity. By utilizing Gi/Gq-DREADDs system via cell-specific viral approach, we achieved precise manipulation of neuronal activity in the motor cortex of CD63-GFP$^{f/+}$ mice. We identified increased neuronal exosome secretion under elevated neuronal activity by investigating the change in CD63-GFP signal. This study provides insight into exosome-mediated communication between neurons and astrocytes and sheds light on the potential role of exosomal signaling in CNS diseases. The use of chemogenetic technology in combination with cell-type-specific reporters provides a powerful tool for investigating exosomal signaling pathways in the CNS.

Table of Contents

List of Figures

List of Abbreviations

AD- Alzheimer’s Disease
CNO- clozapine-N-oxide
DIO- Double-floxed with Inverted Orientation
DREADDs - Designer Receptors Exclusively Activated by Designer Drug
EAAT- excitatory amino acid transporter
EVs- extracellular vesicles
GLT-1- glutamate transporter
GluR - glutamate receptor
GPCRs- G protein-coupled receptors
HD- Huntington’s disease
ILVs- intraluminal vesicles
PD- Parkinson’s Disease

Chapter 1: Introduction

1.1 Communication between neurons and astrocytes

In the nervous system, neurons and astrocytes are two major cell types that are strongly interconnected and rely on mutual communication to support development and synaptic function. During development, neurons modulate astrocyte differentiation through the expression of JAG1 and DLL1, activating Notch signaling(1). With the abundant ion channels and neurotransmitter receptors, astrocyte can respond to neuronal activity quickly and precisely (2). Under the neuron-to-astrocyte communication, astrocyte respond to presynaptic-released neurotransmitters like glutamate with elevation of cytosolic Ca^{2+} (3). The expression of astrocyte synaptic proteins, including glutamate transporter 1 (GLT-1) and excitatory amino acid transporter 2 (EAAT2) (4), and connexins (5), is implicated to be regulated by neuronal glutamatergic activity. To protect neurons from the possible deleterious effects of excessive glutamate concentration, released glutamate from neuronal synapses is taken up via astrocytic glutamate transporters (6). Dysfunctional protection from astrocyte leads to excitotoxicity, which is attributed to the pathogenesis of neurodegenerative diseases such as Alzheimer's Disease (AD) (7), Huntington's disease (HD) (8), and Parkinson's Disease (PD) (9)

1.2 Exosomes and exosome mediated communication

Exosomes, a subtype of bilipid-layer extracellular vesicles (EVs) (10), source from intraluminal vesicles (ILVs) and are released from donor cells during endosomal maturation (11). Endosomal source makes the membrane of exosomes enriched with transport and fusion proteins and tetraspanins (12). Cargo of exosomes includes proteins (e.g., growth factors and transcription factors), nucleic acids (e.g., DNA, mRNAs, miRNAs and lncRNA), and lipids (e.g., sphingomyelin, cholesterol, and ceramide)(13). Due to the property of noninvasively crossing blood-brain barrier without being immunogenic (14), exosomes show the potential as delivery vehicles for biomolecules (15). Recent studies have reported that indirect regulation on neurotransmission via exosomes can contribute to the synapse support, neurite growth and removal, axon regeneration, and neurotransmitter production and recycling (16-18). In neuron-neuron, and neuron-glia communication, neuronal exosomes act as a bridge to modulate the development and function. By transferring glutamate receptor (GluRs) to other neurons via neuronal exosomes, the activation AMPA receptor assembling can be achieved (19). Exosomes from neuronal PC12 cells has been suggested to facilitate synaptic pruning of microglia by enhancing the expression of complement factor C3 (16). In neuron-to-astrocyte communication, astrocytes internalize neuronal exosomes concomitant with upregulated expression of GLT-1 by inhibiting astrocytic miR-124-3p, which protects synapses from exorbitant glutamate level (17). In the pathological conditions of CNS diseases like neurological disorders (20) and neurodegenerative diseases (21), exosomal signaling has been suggested to play an essential role. Synaptic glutamatergic activity of neurons has been suggested to influence the secretion of neuronal exosomes *in vitro* (19,22). What has been remained unexplored is, however, in situ exosomal signaling between neurons and astrocyte in CNS, including the secretion location of exosomes, neuronal activity’s influence on exosome secretion, the recognition and entry mechanisms and downstream regulation in recipient cells.

1.3 Chemogenetic modulation on neuronal activity

In this study, to rigorously investigate the communication between neurons and astrocytes via exosome modulation, we exploited the cell-type specific ILV/exosome reporter and astrocyte reporter CD63-GFP $^{f/+}$ mice, together with chemogenetic technology that allows the expression of Designer Receptors Exclusively Activated by Designer Drug (DREADDs) to achieve precise manipulation of neuronal activity. By utilizing Chemogenetic technique, macromolecules, like G protein-coupled receptors (GPCRs), kinases, and nucleic acid hybrids, can be engineered to interact with previously unrecognized small inactive molecules clozapine analogy clozapine-N-oxide (CNO) (23). CNO-activated DREADDs system, including Gq, Gi, Gs, Golf, and β-arrestin, allows the selective interrogation of GPCR signaling cascades. In Gq-DREADDs system, human M3 muscarinic receptor (hM3) could be mutated to be able to couple with Gαq/11 G protein in order to stimulate phospholipase C, that renders the release of intracellular calcium stores, to achieve the neuronal firing (24). By introducing mutation on human M4 muscarinic receptor (hM4), when coupling with Gαi/o G-protein, the Gi-DREADDs signal can inhibit adenylate cyclase and downstream cAMP production, therefore, to inhibit neuronal signaling (24). In this study, by exploiting Gi/Gq-DREADDs system via cell-specific viral approach, we successfully expressed DREADDs system to neurons in motor cortex and achieved the precise manipulation on neuronal activity on CD63-GFP $^{f/+}$mice. By investigating the change of CD63-GFP signal, we identified the increased neuronal exosome secretion under elevated neuronal activity.

Chapter 2: Methods and Materials

2.1 Animals

The CD63-GFP $^{f/f}$ knock-in mice were generated by homologous recombination. To create the final CD63-copGFP-6xHis targeting vector, the human CD63-copGFP-6xHis cassette was subcloned onto the Rosa-CAG targeting vector downstream of the CAG promoter and upstream of the 3′ arm (17). The CopGFP, a virant of GFP, possesses a very intense fluorescence and is resistant to photobleaching, with no obvious cell toxicity (25). To induce homolog recombination, the targeting vectors were linearized and transfected into the Embryonic Stem (ES) cell line. G418-resistant ES clones were confirmed by Southern blot analysis and implanted into C57BL/6J blastocysts to create chimeric mice following standard procedures. Both ES cell transfections and blastocyst injections were performed by Biocytogen (Worcester, MA). Germline transmission was achieved by breeding chimeric mice with C57BL/6J mice. Male and female mice were used in all experiments, and they were maintained on a 12-hour light/dark cycle with ad libitum access to food and water. All animal care and treatment procedures were strictly carried out in accordance with the NIH Handbook for the Care and Use of Laboratory Animals and the Guidelines for the Use of Animals in Neuroscience Research. The animal techniques utilized in this study were approved by the Tufts University's Institutional Animal Care and Use Committee (IACUC).

2.2 Stereotaxic delivery of AAV and olligos in vivo

The mixture of AAV8-hSyn-DIO-hM3Dq-mCherry (1.5 µL, 3.20 × 10^{13} gc/mL) and AAV9-hSyn-Cre-hGH (0.5 µL, 2.30 × 10^{13} gc/mL) was stereotaxically injected into the motor cortex of right hemisphere of CD63-GFP $^{f/+}$ mice (Bregma 1, X = 1.0 mm, Z = -1.0 mm). The mixture of AAV9-hSyn-Cre-hGH (0.5 µL, 1 × 10^{13} particles/mL) and PBS (1.5 µL, 1X) was stereotaxically injected into the motor cortex of left hemisphere of CD63-

GFP $^{f/+}$ mice (Bregma 1, X = -1.0 mm, Z = -1.0 mm). Mice were anesthetized with isoflurane vapor (w36489, Dschra). Post-operative care included injections of buprenorphine according to the IACUC requirement. Animals were perfused 14 days after injections.

2.3 Drug administration.

Clozapine-N-oxide (CNO) was reconstituted at a concentration of 10 mg/mL in DMSO and subsequently diluted in saline to a final concentration of 0.5 mg/mL for use as a working dosage. The mice received CNO via intraperitoneal injection (i.p.) at a dose of 0.3 mg/kg, two weeks following stereotaxic surgery. The mice were put under CNO-incubaton for 3 hours following injection for investigation of exosome secretion and 1 hour for confirmation of neuronal activity.

2.4 Immunohistochemistry and confocal image acquisition and analysis.

The animals were subjected to deep anesthesia through intraperitoneal injection (IP) of a cocktail of Ketamine (100 mg/kg) and Xylazine (10 mg/kg) in saline. After which, intracardial perfusion with 4% paraformaldehyde (PFA) in PBS was performed. The brains were collected, fixed in 4% PFA at 4 °C overnight, and then cryoprotected in 30% sucrose for 48 hours. Embedding and freezing of brain tissue were accomplished using OCT-Compound Tissu-Tek® (Sakura, Tokyo Japan). Coronal slices (20 μm) were prepared using a cryostat (Leica HM525) and placed on glass SuperFrost Plus slides (Fisher Scientific). For neuronal activity investigation assay, slides were rinsed three times in PBS, then treated with blocking buffer (1% BSA, 5% goat-serum, and 0.2% Triton-X-100 in PBS) for 45 min at room temperature, and incubated with primary antibodies Zif268/Egr1 (1:500, Cell Signaling Technology)at room temperature for 1 hour and then at 4 °C in blocking buffer for 72 hours. Secondary antibody Alexa fluro 633 goat anti-rabbit (Thermo Fisher) was then applied after washing slides three times in PBS.

After incubating under room temperature for 1.5 hour, slides were washed three times in PBS for 5 minutes for each before mounting with ProLong Gold antifade reagent with DAPI (#P36931, Invitrogen). For exosome secretion investigation assay, slides were washed three times in PBS for 5 minutes for each before mounting with ProLong Gold antifade reagent with DAPI (#P36931, Invitrogen). Keyence microscope was used to capture low magnification images at x10 magnification, while confocal images were taken using the Leica Falcon confocal laser scanning microscope (15–20 μm Z-stack with 1.0 μm step) magnified with ×40 (numerical aperture 0.8).

2.5 Signal quantification

For the quantification of CD63-GFP intensity and area in the brain sections, GFP intensity of each Keyence image magnified at 10 × from Green Channel was thresholded to remove background signals after converting to 8-bit type image. The scale of image was set at the micron for unit of length wwith distance in pixels was 0.66. Regions of interest (ROI) for right and left hemesphere on all sections were set before the analysis process respectively. The ROI for right and left hemesphere share the same area value (2406.6 x1327.27 μm^2). The intensity of GFP signal was then measured by ImageJ generating the value of Area, Intergrated Density, and Means. For the quantification of mCherry intensity and area in the brain sections, similar process in CD63-GFP signal quantification was conducted in ImageJ but with new shared ROI value (3260.61 x 2842.42 μm^2) for right and left hemespheres.

For the quantification of the travel distance of exosomes, GFP intensity of each Keyence image (10 ×) from Green Channel was thresholded to remove background signals after converting to 8-bit type image. The tissue areas with thresholeded signals were selected as ROIs for each image before converting the the 8-bit type image to the orginal verison. The tissue area with GFP signal was then measured by using the

Measue function via ImageJ. Same process was applied to quantify the tissue area of mCherry signal via Keyence image (10 ×) from Red Channel.

2.6 Experimental design and statistical analysis.

The sample size and statistical approach employed for each experiment are detailed in the respective method sections and figure legends. GraphPad Prism 7 was utilized to perform all analyses, and individual values were presented for all data. Error bars, where applicable, were represented as S.D. Custom code was not used in the analysis. Variance was analyzed using Two-way analysis of variance (ANOVA), followed by a Tukey post-hoc test for multiple group comparisons. Statistical significance was evaluated at a 95% confidence level ($P < 0.05$), with corresponding P values displayed in each graph.

2.7 Collaboration

The animals for this project are prepared from previous studies in Yang Lab. All the rest methods were conducted by Qiyi Li.

Chapter 3: Results

3.1 Experiment design

To precisely manipulate the neuronal activity, we introduced the Gq-D±READDs system via cell-specific viral approach to neurons in the motor cortex of mice. By exploiting flip-excision(FLEX)-switch approach, also known as Double-floxed with Inverted Orientation (DIO), via viral approach, the DREADDS gene is flanked with two pairs of heterotypic, antiparallel loxP-type recombination sites (Fig. 3.1 A). Because of the inversion of the coding sequence, with the excision of two sites, one of each recombination site will be oppositely oriented and stop the further recombination (23). To drive the expression of cell-specific and Cre-dependent DREADDs, a combination of two neuron-specific encoding viruses (AAV9-hSyn-Cre-hGH; AAV8-hSyn-DIO-hM3Dq-mCherry) were givien to CD63-GFP $^{f/+}$ mice in motor cortex at right hemesphere only (Figure 3.1 C). With the expression of Cre recombinase from AAV9-hSyn-Cre-hGH, the DREADDs expression from AAV8-hSyn-DIO-hM3Dq-mCherry could be turned on.

The tetraspanin family of proteins, including CD81, CD9, and CD63, have been previously identified and validated as specific markers for extracellular vesicles (EVs) and exosomes(26). Notably, CD63, a tetraspanin with minimal expression on the plasma membrane, preferentially labels intracellular endosomal intraluminal vesicles (ILVs)(26).To investigate the change of exosome secretion under increased neuronal activity, Cre-dependent ILV/exosome reporter (CD63-GFP$^{f/f}$) mice were introduced by inserting a loxP-floxed stop codon upstream of human (h) CD63 tagged with copGFP (a GFP variant) and His-tag at its C-terminal. Because both sides of the brain received the AAV9-hSyn-Cre-hGH, CD63-GFP signal can be seen from both hemespheres in both groups (Figure 3.1 C).

Theoretical injection site in longitude is at the bregma (Y= 0 mm), and ± 1.0 mm (X= ± 1.0 mm) to the bregma in latitude, with 1.0 mm depth on each side (Z= -1.0 mm) (Figure 3.1 B). Mice were devided into two groups: Baseline group, and CNO group. Both groups received the same injection of virus, but only CNO group received the intraperitoneal injection (IP) of CNO two weeks after stereotaxic surgery (Figure 3.1 D, E).

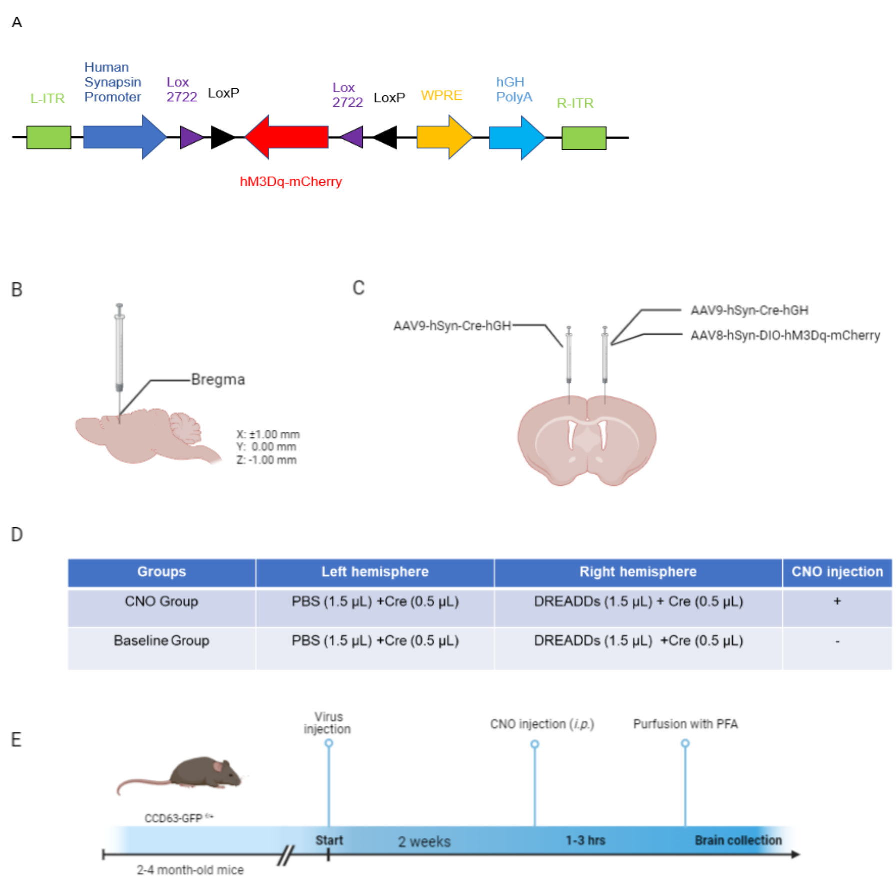

Groups	Left hemisphere	Right hemisphere	CNO injection
CNO Group	PBS (1.5 μL) +Cre (0.5 μL)	DREADDs (1.5 μL) + Cre (0.5 μL)	+
Baseline Group	PBS (1.5 μL) +Cre (0.5 μL)	DREADDs (1.5 μL) +Cre (0.5 μL)	-

Figure 3.1 Experiment design and expression of Gq-DREADDs. (A) Design of the Cre-dependent DIO virus for the expression of hM3Dq-mCherry. (B) Injection site for stereotaxic surgery. (C) Virus injection for each hemisphere of the brain. The right side received the combination of DIO virus (1.5 μL) and Cre virus (0.5 μL), the left side received Cre virus (0.5 μL) diluted in 1 x PBS (1.5 μL). (D) Experiment groups and virus injection. Two groups received same virus injection but only CNO group received CNO via *i.p.* injection. (E) Experiment timeline. CD63-GFP $^{f/+}$ mice were administrated with virus illustrated in (C) via stereotaxic surgery and received CNO via *i.p.* injection after two weeks. The mice were then perfused after 1-3 hours.

3.2 Confirmation of CD63-GFP and DREADDs expression

To confirm the expression of CD63-GFP and DREADDs expression, microscopy from Keyence at x10 magnification was conducted to assess the expression. The brain sections of one mouse from CNO group indicated that CD63-GFP successfully expressed in both hemispheres (Figure 3.2 A, left) and hM3Dq-mCherry expressed only in the right hemisphere (Figure 3.2 A , right). To investigate whether the elevated neuronal exosome secretion is dependent on hM3Dq-mCherry in the londitudinal aspect, we compared the area of mCherry and GFP signal of CD63-GFP$^{f/+}$ mice from the CNO group. We utilized the tissue area of each signal to better represent and compare the distribution of mCherry and CD63-GFP. We artificially set the distance of section with highest tissue area value of mCherry/CD63-GFP as the distance 0, then we ploted following posterior tissue area of two signals (Figure 3.2 C). By looking at the decreasing trend of mCherry and GFP spreading area, it is suggested that the tissue area with mCherry decreased to 0 at 1800 μm, but the GFP area remains around 1 mm^2 at the same side. From following posterior distances after 1800 μm, the GFP signal remained close to 1 mm^2 , even when mCherry signal completely disappreared. This results indicated when the neuronal activity is elevated by Gq-DREADDs system, the secretion of neuronal exosomes is increased but not completely dependent on Gq-DREADDs system because the spreading of exosomes is continuous to the distance where hM3Dq-mCherry expression ends. Figure 3.2 A and B exhibited the GFP and mCherry signal of the section at the distance 0 (true injection site) and distance 1800 μm respectively from Keyence microscopy magnified at x10.

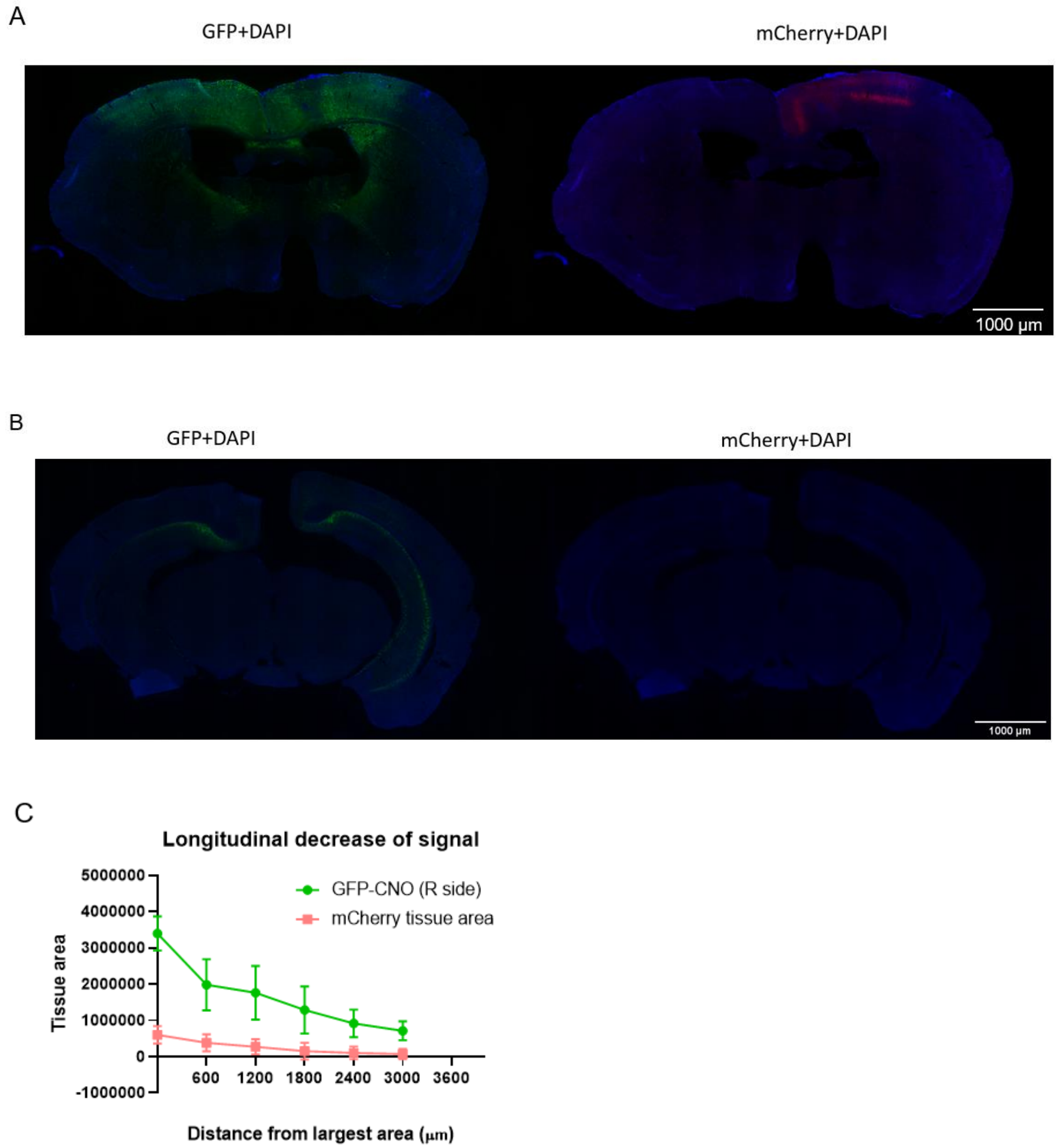

Figure 3.2 Confirmation of the expression and distribution of CD63-GFP and DREADDs. (A) Representative image from Keyence at x10 magnification with Green (GFP) and Blue (DAPI) channels (left) and with Red (mCherry) and Blue (DAPI) channels (right) at injection site and at distance 1800 μm (B). (C) Tissue area of GFP signal mCherry signal on the right side of each section. The distance of section with largest signal area was set as distance 0 (3 mice in this group, 3 slides from each mouse for imaging analysis n=9).

3.3 Neuronal activity assessment

To confirm the activity change of neurons, we investigated the expression of zif268. Zif268 is a transcriptional regulatory progtein of inmmediate early gene that is associated with the neuronal plasticity (27). Confocal microscopy was conducted to assess the immunohisochemical stainning for zif268. Figure 3.3 A shoes the confocal images taken at the injection site, where the CD63-GFP expression was at the similar level in right and left hemisphere of one mice from CNO group. mCherry signal is only observed on the right hemisphere where the DREADDs virus was injected. From the signal of zif268, however, no significant difference of its expression between two sides with different neuronal activity levels was observed. The possible reason of this result could be the area of the brain that we are studying is motor cortex where neurons could be easily activited as long as mice have behaviral activity change.

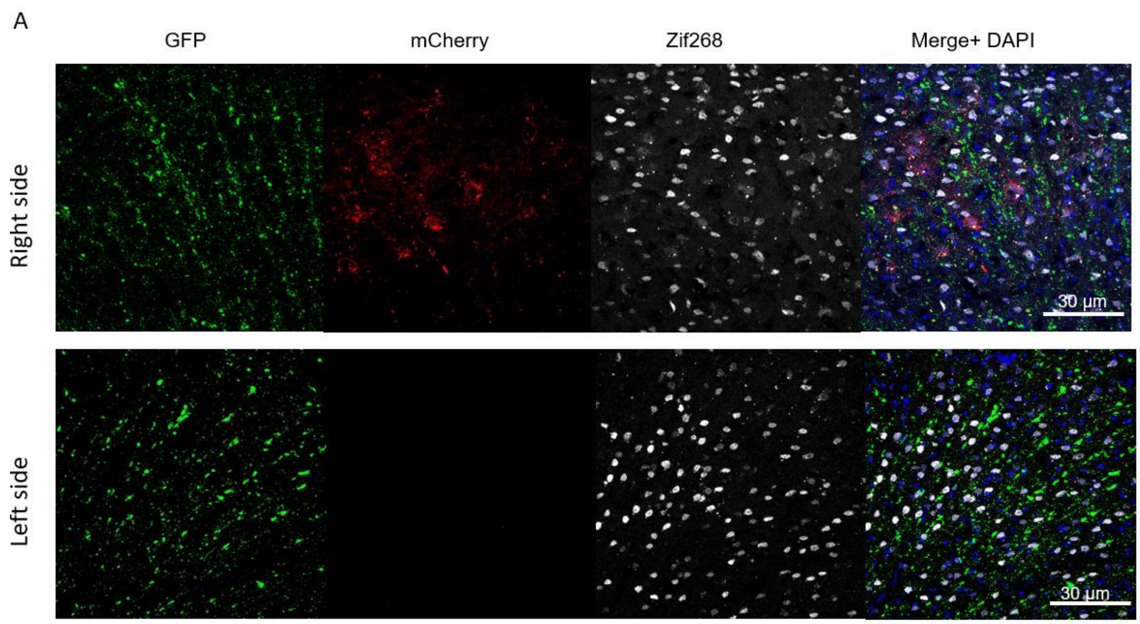

Figure 3.3 Assessment of neuronal activity. (A) Representative confocal images from Leica Falcon at x40 magnification of CD63-GFP $^{f/+}$ mice received CNO. Right hemisphere is the side that received the combination of virus injection. Left hemisphere is the side that received only AAV9-hSyn-Cre-hGH virus. Alexa 633 fluro was the secondary antibody for Zif268.

3.4 Baseline exosome secretion

To compare the exosome secretion between the hemisphere received DREADDs and the hemisphere with Cre virus only from baseline group, quatification of the area and intensity CD63-GFP signal was conducted based on microscopy imgages from Keyence at x10 magnification. Eight longitudinal distances were selected based on the theoretical injection site from 1200 μm anterior to bregma and 3000 μm posterior to bregma with 600 μm between two distances. We artificially set the distance of section with highest CD63-GFP intensity/area on each slide as the distance 0, and its intensity/area as 100%. Then we compared the intensity/area of each section posterior to section at distance 0. Figure 3.4 A and B suggested that both sides exhibit similar trend of decreasing along with the increase of distance (Figure 3.3 C,D) and dropped to near 0% at about 1800 μm. This result meets our hypothesis that without CNO, the Gq-DREADDs system is not activated and, therefore, the similar secretion of neuronal exosomes was generated because neuronal activity in both hemispheres are the same.

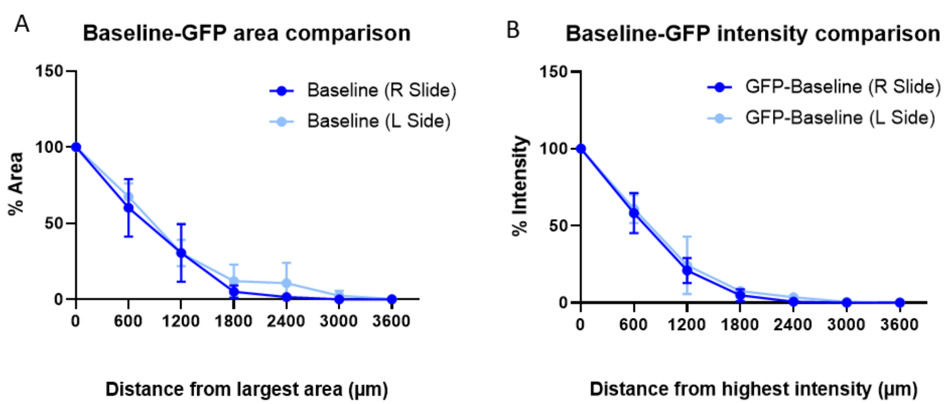

Figure 3.4 Baseline exosome secretion comparison. The distance of section with highest intensity/area was set as the distance 0 and 100% of intensity, every posterior region is compared to this region at distance 0. Comparison of the CD63-GFP area (A) and intensity (B) between the left and right side of the Baseline group (3 mice in this group, 3 slides from each mouse for imaging analysis n=9).

3.5 Elevated exosome secretion

To compare the exosome secretion between the side with elevated neuronal activity (right hemisphere) and normal neuronal activity (left hemisphere), we quantified

CD63-GFP signal of CNO group mice. Similarly, we artificially set the distance of section with highest CD63-GFP intensity/area on each slide as the distance 0, and its intensity/area as 100%. Then we compared the intensity/area of each section posterior to section at distance 0. Two-way ANOVA was used to compare the variance between left and right side in each travel distance point. The CD63-GFP signal intensity in right side reached to near 0% at about 3000 μm. In left side, where no DREADDs is expressed, however, the CD63-GFP signal area decreased to near 0% at around 2400 μm (Figure 3.5 A). Significant difference of CD63-GFP signal area is also observed at distance 600 μm, 1200 μm, and 1800 μm. CD63-GFP signal intensity of right side decreased to near 0% at around 3000 μm, while the intensity of left side decreased to near 0% at about 1800 μm. The significant difference of intensity between two sides is also observed at distance 600 μm and 1200 μm and 1800 μm (Figure 3.5 B).

We specifically compared the area difference between two hemispheres for two groups at the true injection site, 600 μm, and 1200 μm away from true injection site (Figure 3.5 C, E, G). Figure 3.5 C indicated that both hemispheres in two groups share the similar exosome secreiton level at the true injection site, indicating that all four subgroups received the same Cre virus for indicating CD63-GFP. When looking at the exosome secretion level at 600 μm (Figure 3.5 E) and 1200 μm (Figure 3.5 G) away from true injection site, exosome level remained at significant higher level in the right hemisphere of CNO group compared to the rest of three groups. Corresponding representative microscopy images from Keyence microscopy magnified at x10 for CNO and Baseline group were shown in Figure 3.5 D, F, G.

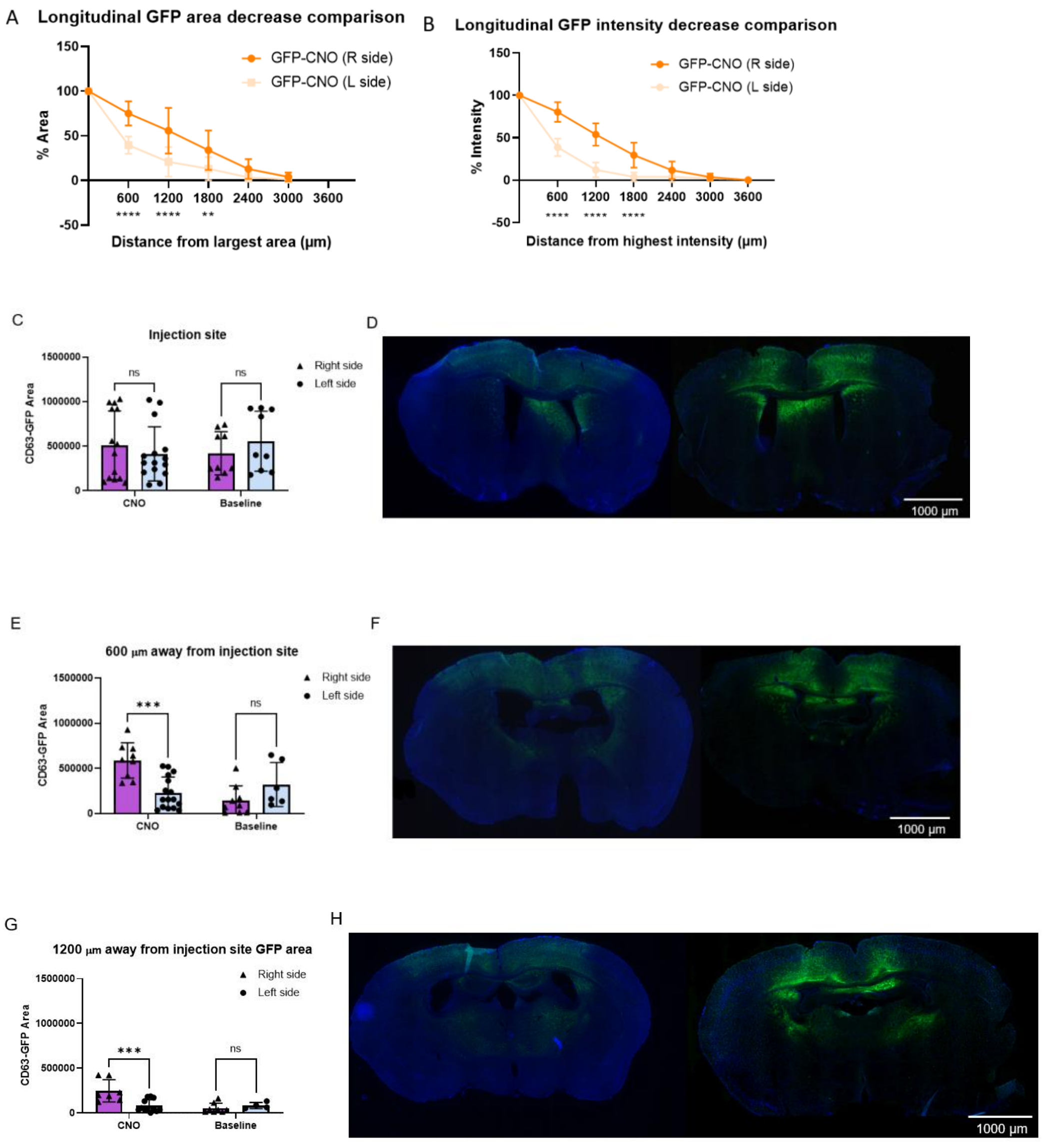

Figure 3.5 Elevated exosome secretion in CNO group and comparison at significant distances. The distance of section with highest intensity/area was set as the distance 0 and 100% of intensity, every posterior region is compared to this region at distance 0. Comparison of the CD63-GFP area (A) and intensity (B) between the lef and right side of the CNO group mice (6 mice in this group, 3 slides from each mouse for imaging analysis, n=18). (C) Comparison of CD63-GFP signal area in right and left sides of mice from CNO and Baseline groups at actual injection site, 600 µm (E), and 1200 µm (G) away from true injection site (sections with highest CD63-GFP area value in each slide). Six mice in CNO group and 3 mice in Baseline group, 3 slides from each mouse for imaging analysis, outliers were excluded. (D) Representative image from Keyence at x10 magnification with Green (GFP) and Blue (DAPI) channels of CNO group (left) and of Baseline group (right) at injection site and 600 µm (F), and 1200 µm (G) away from true injection site. Exposure time of DAPI channel was set higher for CNO group due to the setting issue. *, **, *** and **** indicates $P < 0.05$, $P < 0.01$, $P < 0.001$ and $P < 0.0001$. All error bars reflect s.d.

3.6 Collaboration

All the figures were finished and presented by Qiyi Li

Chapter 4: Discussion

Previous studies on the influence of neuonal activity on its exosomes were mostly based on cultured models and human cerebrospinal fluid (CSF) samples (19,22,28). In this study, we specifically studied the regulation exosomal signaling under elevated neuronal activity in central nervous system (CNS) in situ by expoliting cell-type-specific ILV/exosome and astrocyte reporters in CD63-GFP$^{f/+}$ mice, along with chemogenetic technology. By allowing precisice manipulation on the activity of neurons, chemogenetic technology applied in this study benefited the observation of exosome change in comparison of two hemispheres on the same brain, which reduced the possible errors induced from individual viariance. Our results suggested that when the neuronal activity is elevated above the normal level, the secretion of neuronal exosomes is increased. When looking at the travel distance of the exosomes, our results indicated that, under elevated neuronal activity, the exosomes could still be observed in more posterior region of the brain when compared to the exosomes under normal neuronal activity. In addition, exosomes secretion is continuous even to the distance where the expression of hM3Dq stops. This finding suggested that when neuonal activity is elevated in vivo, it is like that neuronal exosomes travels further than they are under normal condition and could continuously be continuously secreted even when it reaches the further distance where the expression of hM3Dq stops. Our current study shed the light to a preliminary in vivo evidence that supports the previously established notion that exosome secretion is regulated by neuronal activity(19,29). Further studies will focus on the secretion change of exosomes under reduced neuronal activiy with the application of inhibitory Gi-DREADDs system. Analysis of exosomes numbers around astrocytes in more posterior regions with no mCherry signal but CD63-GFP signal on the treatment side at ×63 magnification will also be conducted to confirm the interaction between astrocytes and increased exosomes.

Although similar results were obtained based on both intensity and area analysis, considering the possibility that high intensity in one certain region could be caused by the overlapping of multi-exosomes, or more CD63-GFP proteins expressed on the one exosome, we believe that the resluts based on the analysis of area of CD63-GFP can give a more solid conclusion on the change of exosome secretion. Due to the motor cortex is a region in the brain where neurons could be easily activated as long as animal have behavioral activities during the expriment, it brings the difficulty for us to precisely assess the neuronal activity between two hemisphere via immunohistochemical process.

Taken together, these findings have important implications for our understanding of how exosomes mediate communication between neurons and astrocytes and their potential role in CNS diseases. Our study provides insights into the mechanisms underlying exosomal signaling in the CNS and highlights the potential of chemogenetic technology and cell-type-specific reporters to investigate complex signaling pathways in the CNS. Further exploration of in situ exosomal signaling between neurons and astrocytes could lead to a better understanding of the role of exosomes in the development and progression of CNS diseases. In conclusion, our study highlights the importance of exosomal signaling in the communication between neurons and astrocytes and its potential role in CNS diseases. Further studies are needed to investigate the specific signaling pathways involved in exosomal communication between these cell types and how they may be targeted for therapeutic purposes.

Chapter 5: Bibliography

1. Namihira, M., Kohyama, J., Semi, K., Sanosaka, T., Deneen, B., Taga, T., and Nakashima, K. (2009) Committed neuronal precursors confer astrocytic potential on residual neural precursor cells. *Dev Cell* **16**, 245-255
2. Theodosis, D. T., Poulain, D. A., and Oliet, S. H. R. (2008) Activity-Dependent Structural and Functional Plasticity of Astrocyte-Neuron Interactions. *Physiological Reviews* **88**, 983-1008
3. VERKHRATSKY, A., ORKAND, R. K., and KETTENMANN, H. (1998) Glial Calcium: Homeostasis and Signaling Function. *Physiological Reviews* **78**, 99-141
4. Genoud, C., Quairiaux, C., Steiner, P., Hirling, H., Welker, E., and Knott, G. W. (2006) Plasticity of astrocytic coverage and glutamate transporter expression in adult mouse cortex. *PLoS biology* **4**, e343
5. Koulakoff, A., Ezan, P., and Giaume, C. (2008) Neurons control the expression of connexin 30 and connexin 43 in mouse cortical astrocytes. *Glia* **56**, 1299-1311
6. Pajarillo, E., Rizor, A., Lee, J., Aschner, M., and Lee, E. (2019) The role of astrocytic glutamate transporters GLT-1 and GLAST in neurological disorders: Potential targets for neurotherapeutics. *Neuropharmacology* **161**, 107559
7. Garcia-Esparcia, P., Diaz-Lucena, D., Ainciburu, M., Torrejón-Escribano, B., Carmona, M., Llorens, F., and Ferrer, I. (2018) Glutamate Transporter GLT1 Expression in Alzheimer Disease and Dementia With Lewy Bodies. *Frontiers in aging neuroscience* **10**, 122
8. Petr, G. T., Bakradze, E., Frederick, N. M., Wang, J., Armsen, W., Aizenman, E., and Rosenberg, P. A. (2013) Glutamate transporter expression and function in a striatal neuronal model of Huntington's disease. *Neurochemistry international* **62**, 973-981
9. Mironova, Y. S., Zhukova, I. A., Zhukova, N. G., Alifirova, V. M., Izhboldina, O. P., and Latypova, A. V. (2018) [Parkinson's disease and glutamate excitotoxicity]. *Zhurnal nevrologii i psikhiatrii imeni S.S. Korsakova* **118**, 50-54
10. Tkach, M., and Théry, C. (2016) Communication by Extracellular Vesicles: Where We Are and Where We Need to Go. *Cell* **164**, 1226-1232
11. Colombo, M., Raposo, G., and Théry, C. (2014) Biogenesis, secretion, and intercellular interactions of exosomes and other extracellular vesicles. *Annual review of cell and developmental biology* **30**, 255-289
12. Vlassov, A. V., Magdaleno, S., Setterquist, R., and Conrad, R. (2012) Exosomes: current knowledge of their composition, biological functions, and diagnostic and therapeutic potentials. *Biochimica et biophysica acta* **1820**, 940-948
13. Xia, X., Wang, Y., Qin, Y., Zhao, S., and Zheng, J. C. (2022) Exosome: A novel neurotransmission modulator or non-canonical neurotransmitter? *Ageing Research Reviews* **74**, 101558
14. Alvarez-Erviti, L., Seow, Y., Yin, H., Betts, C., Lakhal, S., and Wood, M. J. A. (2011) Delivery of siRNA to the mouse brain by systemic injection of targeted exosomes. *Nature Biotechnology* **29**, 341-345
15. Osier, N., Motamedi, V., Edwards, K., Puccio, A., Diaz-Arrastia, R., Kenney, K., and Gill, J. (2018) Exosomes in Acquired Neurological Disorders: New Insights into Pathophysiology and Treatment. *Molecular Neurobiology* **55**, 9280-9293
16. Bahrini, I., Song, J.-h., Diez, D., and Hanayama, R. (2015) Neuronal exosomes facilitate synaptic pruning by up-regulating complement factors in microglia. *Scientific reports* **5**, 7989

17. Men, Y., Yelick, J., Jin, S., Tian, Y., Chiang, M. S. R., Higashimori, H., Brown, E., Jarvis, R., and Yang, Y. (2019) Exosome reporter mice reveal the involvement of exosomes in mediating neuron to astroglia communication in the CNS. *Nature communications* **10**, 4136
18. Prada, I., Gabrielli, M., Turola, E., Iorio, A., D'Arrigo, G., Parolisi, R., De Luca, M., Pacifici, M., Bastoni, M., and Lombardi, M. (2018) Glia-to-neuron transfer of miRNAs via extracellular vesicles: a new mechanism underlying inflammation-induced synaptic alterations. *Acta neuropathologica* **135**, 529-550
19. Lachenal, G., Pernet-Gallay, K., Chivet, M., Hemming, F. J., Belly, A., Bodon, G., Blot, B., Haase, G., Goldberg, Y., and Sadoul, R. (2011) Release of exosomes from differentiated neurons and its regulation by synaptic glutamatergic activity. *Molecular and Cellular Neuroscience* **46**, 409-418
20. Osier, N., Motamedi, V., Edwards, K., Puccio, A., Diaz-Arrastia, R., Kenney, K., and Gill, J. (2018) Exosomes in Acquired Neurological Disorders: New Insights into Pathophysiology and Treatment. *Mol Neurobiol* **55**, 9280-9293
21. Quek, C., and Hill, A. F. (2017) The role of extracellular vesicles in neurodegenerative diseases. *Biochemical and biophysical research communications* **483**, 1178-1186
22. Fauré, J., Lachenal, G., Court, M., Hirrlinger, J., Chatellard-Causse, C., Blot, B., Grange, J., Schoehn, G., Goldberg, Y., Boyer, V., Kirchhoff, F., Raposo, G., Garin, J., and Sadoul, R. (2006) Exosomes are released by cultured cortical neurones. *Molecular and Cellular Neuroscience* **31**, 642-648
23. Urban, D. J., and Roth, B. L. (2015) DREADDs (Designer Receptors Exclusively Activated by Designer Drugs): Chemogenetic Tools with Therapeutic Utility. *Annual Review of Pharmacology and Toxicology* **55**, 399-417
24. Armbruster, B. N., Li, X., Pausch, M. H., Herlitze, S., and Roth, B. L. (2007) Evolving the lock to fit the key to create a family of G protein-coupled receptors potently activated by an inert ligand. *Proc Natl Acad Sci U S A* **104**, 5163-5168
25. Shagin, D. A., Barsova, E. V., Yanushevich, Y. G., Fradkov, A. F., Lukyanov, K. A., Labas, Y. A., Semenova, T. N., Ugalde, J. A., Meyers, A., Nunez, J. M., Widder, E. A., Lukyanov, S. A., and Matz, M. V. (2004) GFP-like proteins as ubiquitous metazoan superfamily: evolution of functional features and structural complexity. *Mol Biol Evol* **21**, 841-850
26. Andreu, Z., and Yáñez-Mó, M. (2014) Tetraspanins in extracellular vesicle formation and function. *Front Immunol* **5**, 442
27. Knapska, E., and Kaczmarek, L. (2004) A gene for neuronal plasticity in the mammalian brain: Zif268/Egr-1/NGFI-A/Krox-24/TIS8/ZENK? *Progress in Neurobiology* **74**, 183-211
28. Street, J. M., Barran, P. E., Mackay, C. L., Weidt, S., Balmforth, C., Walsh, T. S., Chalmers, R. T., Webb, D. J., and Dear, J. W. (2012) Identification and proteomic profiling of exosomes in human cerebrospinal fluid. *Journal of translational medicine* **10**, 5
29. Ataman, B., Ashley, J., Gorczyca, M., Ramachandran, P., Fouquet, W., Sigrist, S. J., and Budnik, V. (2008) Rapid activity-dependent modifications in synaptic structure and function require bidirectional Wnt signaling. *Neuron* **57**, 705-718